

Article

Topological Model of an Electromagnetic Environment Inside a Ship for Electromagnetic Compatibility (EMC) Analysis

Ryszard J. Katulski ^{1,*} and Rafał Namiotko ²

¹ Faculty of Electronics, Telecommunications and Informatics, Gdansk University of Technology, 80-233 Gdansk, Poland

² R&D Marine Technology Centre, 81-109 Gdynia, Poland; rafal.namiotko@ctm.gdynia.pl

* Correspondence: ryszard.katulski@eti.pg.edu.pl

Received: 19 September 2019; Accepted: 6 October 2019; Published: 12 October 2019



Abstract: The mutual electromagnetic (EM) interactions between electrical and electronic devices in a segmented space, such as a ship's environment, are described. Knowledge of EM interference signal (EM disturbance) distribution is important when setting correct locations for electrical and electronic equipment in a ship's environment. Firstly, the topological structure of a ship's segmented internal environment (under the main deck), which consists of many electrical screening walls (shielding planes), is presented. The planes attenuate the EM disturbances. Then, taking into account the ship's topological structure, a general description of the EM disturbance distribution, called the ship's topological electromagnetic compatibility (EMC) model, is formulated using matrix expressions. This model includes EM disturbances that radiate from a ship's own internal sources (located under the main deck) and/or external sources (located above the main deck), and/or that radiate from extraneous external sources, i.e., from other ships and/or aircrafts. A description of the model for an example EMC ship scenario and a partial verification of its measurements are shown and discussed. Finally, a discussion of the usefulness of the proposed model in an analysis of a ship's EMC conditions concludes this study.

Keywords: EM interactions; protection before EM influences; EMC; EMC investigations; EM signals (disturbances) on a ship; EM shielding walls; EM disturbance attenuation; EM disturbance distributions; topological modeling; matrix description; practical scenarios; measurement verification

1. Introduction

The subject of this article is a software expert system for the analysis of the electromagnetic compatibility (EMC) conditions on a ship as a tool to support the design, exploitation, and modernization of sea vessel equipment, especially in navy ships. This system can be used to analyze the EMC of not only a ship's environment, but also other topological structures. This subject is very important in practice; however, for defense reasons, it is not widely described in the scientific and technical literature.

The idea of a topological description of the field interactions between electrical and electronic elements and systems was proposed by Tesche [1]. This approach was developed by Baum [2], Parmantier et al. [3], and Agee et al. [4]. The phrase "topological" means the type of spatial object; in this case, it characterizes the ship structure, especially the internal structure (below the deck). A ship's construction is a complicated spatial structure with a specified number of electromagnetic (EM) shielding walls, such as decks, superstructures, compartments, and rooms through which EM disturbances penetrate and influence the functioning of the ship's electrical and electronic devices. On the other hand, the shielding walls also perform useful functions, particularly in the protection of the

ship's steering systems and control networks against disturbances. To improve the EMC conditions, it is desirable to effectively lower the level of the disturbances that affect the electrical and electronic devices and systems, as well as the radiation from them [5]. Another important problem to consider is the EM leak of information, which degrades the safety and security conditions of the ship's information system [6].

For many years, problems related to the state of the EMC conditions in a ship's environment have been the subject of joint research conducted at the Gdansk University of Technology's and at the R&D Marine Technology Centre in Gdynia (Poland) [7].

The design of a ship's internal structure and deployment of electrical and electronic devices is a complex problem due to the fact that the signals from these devices negatively influence each other's operations. This is a very important problem to consider in naval ships. It is known that every ship contains different electrical, electronic, and radio devices, including electrical power equipment and transmitting antennas, that radiate EM fields (EM disturbances), which influence the operation and functionality of the electrical and electronic equipment. Moreover, naval ships have many command and steering systems composed of different electronic elements. Additionally, due to the complicated form of a ship's structure, which consists of many EM shielding walls, investigations into the EMC conditions of the ship's internal environment, i.e., under the main deck, is a very complex issue. Knowledge of the EMC condition state of a ship's environment improves design procedures, exploitation efficiency, and modernization tasks in the ship. The proposed topological EMC model and its matrix description can be used to improve EMC analysis.

The described method for analyzing EMC conditions when designing the ship's internal structure, the deployment of energy stations, radio communication and radio navigation equipment, and elements of the ship's control systems has important utility. The described method also has use during the performance of modernization work on a ship's equipment, e.g., installing new electronic systems that are necessary on the modern battlefield.

One novelty of this article is the use of a matrix calculus to describe the distribution of EM disturbances in a ship's topological structure. Using such an approach to analyze the state of the EMC condition of the electrical and electronic systems and devices installed in such structures, an effective computational tool was developed for practical applications.

The problem outlined in this paper is based on the theory and practice of EM shielding, and takes into account applicable standards [8–11]. First, the topological model of a typical ship's construction with the shielding planes is shown and the EM disturbance sources are classified. Next, the matrix description of the EMC model is formulated. The description of a general EMC scenario using the model is also presented. To verify the assumptions, the results of calculations and measurements obtained under in situ conditions are compared and analyzed. Finally, the practical usefulness of the topological model for investigations into the EMC conditions of a ship's environment are summarized.

2. The Concept of an EMC Topological Model

It should be emphasized that the proposed model is intended for numerical calculations used in simulations of various interference scenarios reflecting situations occurring during ship's operation. This involves calculating the effective RMS (Root Mean Square) value corresponding to the value measured with a broadband electric field meter at the indicated place on the ship. The value of the electromagnetic interference (e-m) is determined by the electrical component of this interference, which is expressed by Equations (1)–(5).

Estimating this value is very useful both in the initial design analyses and also in the specific operating conditions of the ship. The sources of this interference are usually radiocommunication and radiolocation transmitters, as well as intentional e-m signals coming from different sources. This makes it possible to predict threats to the ship's operation devices resulting from such disturbances and, on this basis, to protect these devices using appropriate shielding and/or appropriate locations in the ship's structure. The most susceptible systems to such disturbances are automatic ship command

systems, especially certain elements of this system, e.g., the torpedo tube control subsystem. For obvious reasons, the details of this are not the subject of the reviewed article. For this reason, the topological model presented in the article as described by matrix equations was presented at a high level of generality when expressing the idea of these calculations. In these simulations, only the attenuation of the ship's walls and attenuation in the spaces between these walls were taken into account, which are described in detail below (p. 2.2).

In addition, the applied description of the propagation of interference from their sources to the indicated place on the ship was not rigorous; it was not based on a vector description and was not of a waveform nature. This approach would be virtually impossible in such dynamic conditions on the ship.

2.1. A Ship's EMC Topological Structure

As already mentioned, a typical ship structure consists of a specified number of shielding walls, i.e., shielding planes, that influence the EM disturbance distribution. A disturbance interaction of an EM signal is related to its electrical component E , i.e., the electrical field strength. In practice, the disturbance distribution is described by effective values of the electrical component E of the propagating EM field, which mainly depends on the localization and value of its source and the properties of the shielding planes. The arrangement of the shielding planes results from the ship's internal structure. Figure 1 shows a ship's general topological structure, where:

- EuT is the equipment under test that is affected by all existing disturbing signals;
- S_p is the p -th shielding plane, such as a deck or walls, and $p \in (1, 2, \dots, P)$;
- $D_m^{(i)}$ is the m -th internal (i.e., under the main deck) EM field source (disturbance source) that radiates the $E_m^{(i)}$ disturbing signal, where $m \in (1, 2, \dots, M)$;
- $D_j^{(o)}$ is the j -th external (i.e., above the main deck) EM field source (disturbance source) that radiates the $E_j^{(o)}$ disturbing signal, where $j \in (1, 2, \dots, J)$; and
- $D_k^{(e)}$ is the k -th extraneous external EM field source (disturbance source) that radiates the $E_k^{(e)}$ disturbing signal from another ship or aircraft, where $k \in (1, 2, \dots, K)$.

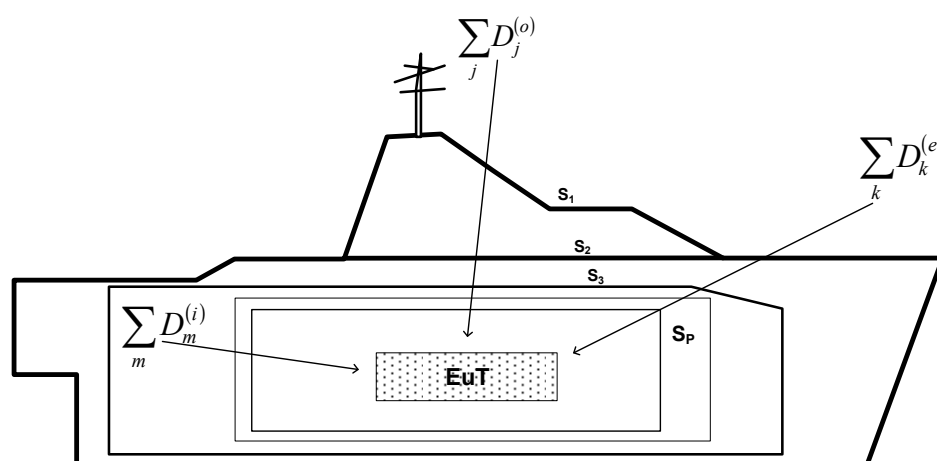


Figure 1. The topological form of a ship's structure with shielding planes (walls), S , and electromagnetic (EM) disturbance sources, D , equipment under test (EuT).

Using the above-presented topological structure of a ship's environment, the value of the total disturbing signal at a given equipment under test (EuT) device, taking into account the arrangement of the signal sources and the location of particular shielding planes, can be calculated. An effective value $E_l^{(t)}$ of the total disturbing signal at the selected l -th EuT can be calculated in the following way,



due to the resultant disturbing signals that are radiated by transmitting antennas, with other sources of disturbing signals being classified into three groups, namely, internal, external, and extraneous external, i.e.,

$$E_l^{(t)} = \sqrt{\left(E_l^{(i)}\right)^2 + \left(E_l^{(o)}\right)^2 + \left(E_l^{(e)}\right)^2}, \quad (1)$$

in which

- $E_l^{(i)}$ is the resultant value of the sum of the ship's own internal disturbing signals, which equals

$$E_l^{(i)} = \sqrt{\sum_{m=1}^M \left(E_{lm}^{(i)}\right)^2}, \quad (2)$$

- $E_l^{(o)}$ is the resultant value of the sum of the ship's own external disturbing signals, which equals

$$E_l^{(o)} = \sqrt{\sum_{j=1}^J \left(E_{lj}^{(o)}\right)^2}, \quad (3)$$

- $E_l^{(e)}$ is the resultant value of the sum of extraneous external disturbing signals, which equals

$$E_l^{(e)} = \sqrt{\sum_{k=1}^K \left(E_{lk}^{(e)}\right)^2}. \quad (4)$$

Equations (1)–(4) describe the summation of disturbing signals, which indicate the measured effective scalar quantities; these powers are expressed by squares of electric field strength of the electromagnetic signal.

As can be seen, the disturbing signal values depend on their source values, the space attenuation of the disturbing signals along the paths between their sources and the EuT's location, and the attenuation of the shielding planes that are located on the propagation paths of the disturbance signals.

Otherwise, the total value of $E_l^{(t)}$ does not exceed its accepted (limited) value of $E_{l(\text{lim})}^{(t)}$, ensuring the correct operation of the l -th EuT, i.e.,

$$E_l^{(t)} \leq E_{l(\text{lim})}^{(t)}. \quad (5)$$

Verification of Equation (5) is one of the main goals of EMC analysis. This requires calculating the abovementioned sums of the disturbing signals, i.e., $E_l^{(i)}$, $E_l^{(o)}$, and $E_l^{(e)}$, for which the topological model of the ship's EMC environment is proposed. However, if the total value $E_l^{(t)}$ of the disturbing signals at the EuT device exceeds the threshold value $E_{l(\text{lim})}^{(t)}$, an additional shielding cover to suppress the disturbing signals should be used.

2.2. The Matrix Description of the EMC Topological Model

Considering the topological model of a ship's structure, we can determine the effective value of $E_l^{(t)}$ —the resultant EM disturbance that influences the operation of the selected l -th EuT—as presented in Figure 1 and described by Equation (1). The value of the first component $E_l^{(i)}$ in Equation (1), i.e.,



the components $E_{lm}^{(i)}$ in Equation (2), where $m \in 1, 2, \dots, M$, can be calculated by solving the following matrix equation:

$$\begin{aligned} \begin{bmatrix} E_{l1}^{(i)} \\ E_{l2}^{(i)} \\ \cdot \\ E_{lm}^{(i)} \\ \cdot \\ E_{lM}^{(i)} \end{bmatrix} &= \begin{bmatrix} E_{l1}^{(i)} \\ E_{l2}^{(i)} \\ \cdot \\ E_{lm}^{(i)} \\ \cdot \\ E_{lM}^{(i)} \end{bmatrix} \\ &= [d^{(i)}]_{M \times M} \cdot [E^{(i)}(0)]_{M \times 1} - \sum_{i=1}^M \left(\left([sc^{(i)}]_{M \times P} \cdot [a_w^{(i)}]_{P \times M} \right), [E_{ii}]_{M \times M} \right) \cdot [e_i]_{M \times 1} - [a_s^{(i)}]_{M \times 1}, \end{aligned} \tag{6}$$

in which

- $[d^{(i)}]_{M \times M}$ is a diagonal matrix of the activation coefficients of the ship's own internal disturbance sources, which can be used to activate the selected sources of the disturbing signals in simulation investigations, i.e., the matrix has the following form:

$$[d^{(i)}]_{M \times M} = \begin{bmatrix} d_1^{(i)} & \dots & \dots & \dots & \dots & \dots \\ \dots & d_2^{(i)} & \dots & \dots & \dots & \dots \\ \dots & \dots & \dots & \dots & \dots & \dots \\ \dots & \dots & \dots & d_m^{(i)} & \dots & \dots \\ \dots & \dots & \dots & \dots & \dots & \dots \\ \dots & \dots & \dots & \dots & \dots & d_M^{(i)} \end{bmatrix}, \text{ where } d_m^{(i)} = \begin{cases} 1, & \text{if } D_m^{(i)} \text{ is active,} \\ 0, & \text{if } D_m^{(i)} \text{ is not active;} \end{cases} \tag{7}$$

- $[E^{(i)}(0)]_{M \times 1}$ is a vector of the source values of the ship's own internal disturbing signals, which has the following form:

$$[E^{(i)}(0)]_{M \times 1} = \begin{bmatrix} E_1^{(i)}(0) \\ E_2^{(i)}(0) \\ \cdot \\ E_m^{(i)}(0) \\ \cdot \\ E_M^{(i)}(0) \end{bmatrix}, \tag{8}$$

where $E_m^{(i)}(0)$ is the value of the m -th source's disturbing signal;

- $[sc^{(i)}]_{M \times P}$ is a matrix of the presence coefficients of the shielding planes in the propagation.

Path of the ship’s own internal disturbing signals, which has the following form:

$$[sc^{(i)}]_{M \times P} = \begin{bmatrix} SC_{11} & SC_{12} & \dots & SC_{1p} & \dots & SC_{1P} \\ SC_{21} & SC_{22} & \dots & SC_{2p} & \dots & SC_{2P} \\ \dots & \dots & \dots & \dots & \dots & \dots \\ SC_{m1} & SC_{m2} & \dots & SC_{mp} & \dots & SC_{mP} \\ \dots & \dots & \dots & \dots & \dots & \dots \\ SC_{M1} & SC_{M2} & \dots & SC_{Mp} & \dots & SC_{MP} \end{bmatrix}, \tag{9}$$

where

$$sc_{mp} = \begin{cases} 1, & \text{if } m\text{-th disturbance is attenuated by } p\text{-th shielding plane,} \\ 0, & \text{if } m\text{-th disturbance is not attenuated by } p\text{-th shielded plane;} \end{cases} \tag{10}$$

- $[a_w^{(i)}]_{P \times M}$ is a matrix of the attenuation values of the ship’s own internal disturbing signals when passing through the shielding planes, which has the following form:

$$[a_w^{(i)}]_{P \times M} = \begin{bmatrix} a_{w11}^{(i)} & a_{w12}^{(i)} & \dots & a_{w1p}^{(i)} & \dots & a_{w1M}^{(i)} \\ a_{w21}^{(i)} & a_{w22}^{(i)} & \dots & a_{w2p}^{(i)} & \dots & a_{w2M}^{(i)} \\ \dots & \dots & \dots & \dots & \dots & \dots \\ a_{wp1}^{(i)} & a_{wp2}^{(i)} & \dots & a_{wpm}^{(i)} & \dots & a_{wpM}^{(i)} \\ \dots & \dots & \dots & \dots & \dots & \dots \\ a_{wP1}^{(i)} & a_{wP2}^{(i)} & \dots & a_{wPm}^{(i)} & \dots & a_{wPM}^{(i)} \end{bmatrix}, \tag{11}$$

where $a_{wpm}^{(i)}$ is the attenuation value of the p -th shielding plane for the frequency of the m -th internal disturbing signal $E_m^{(i)}$.

- $\langle a, b \rangle$ is the Frobenius inner product in the form of the sum of the Hadamard product elements [12];
- $[E_{ii}]$ is a matrix with “1” in the “ii” position and “0” in the other positions;
- $[e_i]$ is a vector with “1” in the “i” position and “0” in the other positions;
- $[a_s^{(i)}]_{M \times 1}$ is a vector of the space attenuation values of the disturbing signals along their propagation path from sources to the EuT, which has the following form:

$$[a_s^{(i)}]_{M \times 1} = \begin{bmatrix} a_{s1}^{(i)} \\ a_{s2}^{(i)} \\ \cdot \\ \cdot \\ a_{sm}^{(i)} \\ \cdot \\ \cdot \\ a_{sM}^{(i)} \end{bmatrix}, \tag{12}$$

where $a_{sm}^{(i)}$ is the space attenuation value of the m -th internal disturbing signal that can be calculated or measured.

The attenuation a_w of a shielding plane (wall) depends on the disturbing signal’s frequency f , the shielding material’s thickness h , and its kind, i.e., its conductivity σ and relative magnetic permeability

μ . In practice, the attenuation value is calculated or measured at the given frequencies [13]. The results of this can be recorded in matrix form, i.e., $\left[a_w^{(i)} \right]$.

The values of the other components included in Equation (1), i.e., $E_l^{(o)}$ and $E_l^{(e)}$, should be calculated in a similar way to (6)–(12), i.e.,

$$\begin{aligned} \left[E_l^{(o)} \right] &= \begin{bmatrix} E_{l1}^{(o)} \\ E_{l2}^{(o)} \\ \cdot \\ E_{lj}^{(o)} \\ \cdot \\ E_{lJ}^{(o)} \end{bmatrix} \\ &= \left[d^{(o)} \right]_{J \times J} \cdot \left[E^{(o)}(0) \right]_{J \times 1} - \sum_{i=1}^J \left(\left(\left[sc^{(o)} \right]_{J \times P} \cdot \left[a_w^{(o)} \right]_{P \times J} \right), \left[E_{ii} \right]_{J \times J} \right) \left[e_i \right]_{J \times 1} - \left[a_s^{(o)} \right]_{J \times 1} \end{aligned} \tag{13}$$

in which

- $\left[d^{(o)} \right]_{J \times J}$ is a diagonal matrix of the activation coefficients of the ship’s own external disturbing sources, which has the same role as and a similar form to Equation (7);
- $\left[E^{(o)}(0) \right]_{J \times 1}$ is a vector of the source values of the ship’s own external disturbing signals, which has a similar form to Equation (8);
- $\left[sc^{(o)} \right]_{J \times P}$ is a matrix of the presence coefficients of the shielding planes on the propagation path of the ship’s own internal disturbing signals, which has a similar form to Equation (9);
- $\left[a_w^{(o)} \right]_{P \times J}$ is a matrix of the loss (attenuation) values of the ship’s own external disturbing signals when passing through the shielding planes, which has a similar form to Equation (11);
- $\left[a_s^{(o)} \right]_{J \times 1}$ is a vector of the space attenuation values of the disturbing signals along their propagation path from sources to the EuT, which has a similar form to Equation (12) and

$$\begin{aligned} \left[E_l^{(e)} \right] &= \begin{bmatrix} E_{l1}^{(e)} \\ E_{l2}^{(e)} \\ \cdot \\ E_{lk}^{(e)} \\ \cdot \\ E_{lK}^{(e)} \end{bmatrix} \\ &= \left[d^{(e)} \right]_{K \times K} \cdot \left[E^{(e)}(0) \right]_{K \times 1} - \sum_{i=1}^K \left(\left(\left[sc^{(e)} \right]_{K \times P} \cdot \left[a_w^{(e)} \right]_{P \times K} \right), \left[E_{ii} \right]_{K \times K} \right) \left[e_i \right]_{K \times 1} - \left[a_s^{(e)} \right]_{K \times 1} \end{aligned} \tag{14}$$

in which

- $\left[d^{(e)} \right]_{K \times K}$ is a diagonal matrix of the activation coefficients of the extraneous external disturbing sources, which has the same role as and a similar form to Equation (7);
- $\left[E^{(e)}(0) \right]_{K \times 1}$ is a vector of the source values of the extraneous external disturbing signals, which has a similar form to Equation (8);

- $[sc^e]_{K \times P}$ is a matrix of the presence coefficients of the shielding planes on the path of the extraneous external disturbing signals, which has the same form as Equation (9);
- $[a_w^{(e)}]_{P \times K}$ is a matrix of the loss (attenuation) values of the extraneous external disturbing signals when passing through the shielding planes, which has a similar form to Equation (11);
- $[a_s^{(e)}]_{K \times 1}$ is a vector of the space attenuation values of the extraneous external disturbing signals along their propagation path from sources to the EuT, which has a similar form to Equation (12).

The above also require knowledge of the remaining vectors and matrices, i.e., $[d^{(o)}]_{J \times J'}$, $[d^{(e)}]_{K \times K'}$, $[E_j^{(o)}(0)]_{J \times 1}$, $[E_k^{(e)}(0)]_{K \times 1}$, $[sc^{(o)}]_{J \times P'}$, $[sc^{(e)}]_{K \times P'}$, $[a_w^{(o)}]_{P \times J'}$, $[a_w^{(e)}]_{P \times K'}$, $[a_s^{(o)}]_{J \times 1}$, and $[a_s^{(e)}]_{K \times 1}$, which can be formulated in the above-described way.

3. Description of the General EMC Topological Model

3.1. General Scenario

A practical application of the described EMC topological model is presented in the general scenario illustrated in Figure 2, where the ship's structure consists of four shielding planes S_{1-4} and the given EuT is located in a cabin (shielding plane S_4). Four internal disturbing signals, five external disturbing signals, and seven extraneous external disturbing signals radiate from their sources $D_{m=1 \div 4}^{(i)}$, $D_{j=1 \div 5}^{(o)}$ and $D_{k=1 \div 7}^{(e)}$, and have an influence on the operation of the EuT.

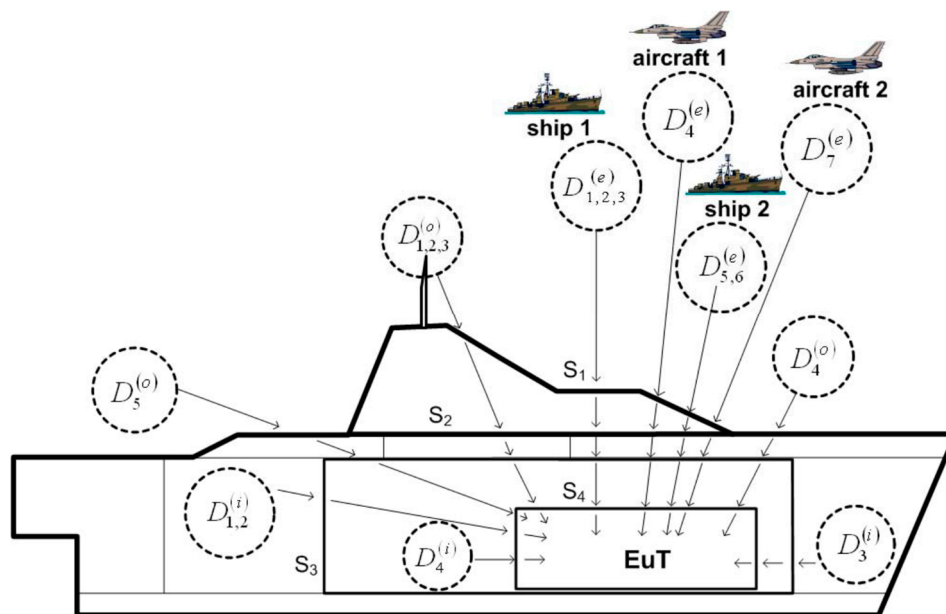


Figure 2. The general scenario of the disturbance source locations.

These disturbing signals can be characterized as follows.

- Firstly, the ship's own internal disturbance sources are:
 - $D_1^{(i)}$, the ship's power station, which radiates the disturbing signal $E_1^{(i)}$, propagating to the EuT via shielding planes S_3 and S_4 ;
 - $D_2^{(i)}$, the ship's power system, which radiates the disturbing signal $E_2^{(i)}$, propagating to the EuT via shielding planes S_3 and S_4 ;



- $D_3^{(i)}$, the ship's passive defense system, which radiates the disturbing signal $E_3^{(i)}$, propagating to the EuT also via shielding planes S_3 and S_4 ;
 - $D_4^{(i)}$, the ship's radio station, which radiates the disturbing signal $E_4^{(i)}$, propagating to the EuT only via shielding plane S_4 .
- Secondly, the ship's own external disturbance sources are:
 - $D_1^{(o)}$, the ship's navigation radar antenna, which radiates the disturbing signal $E_1^{(o)}$, propagating to the EuT via all shielding planes;
 - $D_2^{(o)}$, the ship's combat radar antenna, which radiates the disturbing signal $E_2^{(o)}$, propagating to the EuT via all shielding planes;
 - $D_3^{(o)}$, the ship's high-frequency (HF) radio station transmitting antenna, which radiates the disturbing signal $E_3^{(o)}$, propagating to the EuT via all shielding planes;
 - $D_4^{(o)}$, the ship's active defense system, which radiates the disturbing signal $E_4^{(o)}$, propagating to the EuT via shielding planes S_2 , S_3 , and S_4 ; and
 - $D_5^{(o)}$, the ship's helicopter, which radiates the disturbance signal $E_5^{(o)}$, propagating to the EuT also via shielding planes S_2 , S_3 , and S_4 .
 - Thirdly, the extraneous disturbance sources are:
 - $D_1^{(e)}$, the transmitting antenna of the combat radar equipment for the first extraneous ship, which radiates the disturbing signal $E_1^{(e)}$, propagating to the EuT via all shielding planes;
 - $D_2^{(e)}$, the navigation radar antenna of the first extraneous ship, which radiates the disturbing signal $E_2^{(e)}$, propagating to the EuT via all shielding planes;
 - $D_3^{(e)}$, the transmitting antenna of the very-high-frequency (VHF) radio station of the first extraneous ship, which radiates the disturbing signal $E_3^{(e)}$, propagating to the EuT via all shielding planes;
 - $D_4^{(e)}$, the transmitting antenna of the ultra-high-frequency (UHF)/VHF station of the first extraneous combat aircraft, which radiates the disturbing signal $E_4^{(e)}$, propagating to the EuT via all shielding planes;
 - $D_5^{(e)}$, the navigation radar antenna of the second extraneous ship, which radiates the disturbing signal $E_5^{(e)}$, propagating to the EuT via all shielding planes;
 - $D_6^{(e)}$, the transmitting antenna of the navigation radar equipment of the second extraneous ship, which radiates the disturbing signal $E_6^{(e)}$, propagating to the EuT via all shielding planes;
 - $D_7^{(e)}$, the transmitting antenna of the navigation radar equipment of the second extraneous combat aircraft, which radiates the disturbing signal $E_7^{(e)}$, propagating to the EuT via all shielding planes.

The method for preparing the contents of the matrices and vectors in Equation (6), Equation (13), and Equation (14) for the scenario shown in Figure 2 is presented in Section 3.2.

3.2. Description of the Topological Matrix

As already mentioned, the main subject of EMC condition investigations of a ship's environment during its design and exploitation in practice involves determining the resultant value of the disturbing signal, as seen in Equation (1), at the selected EuT device. As shown in Figure 2, the resultant disturbance is the sum of three classes of disturbances, i.e., internal, external, and extraneous disturbances. Each

group consists of a specified number of disturbing signals. The internal group contains four disturbing signals, the external group contains five disturbing signals, and the extraneous group contains seven disturbing signals, i.e., $E_{m=1\div 4}^{(i)}$, $E_{j=1\div 5}^{(o)}$ and $E_{k=1\div 7}^{(e)}$, respectively. To calculate the resultant value in Equation (1) of the total disturbing signal $E_l^{(t)}$ at the selected l -th EuT, the values of Equations (2)–(4), i.e., $E_l^{(i)}$, $E_l^{(o)}$, and $E_l^{(e)}$, are calculated. Thus, it is necessary to have knowledge of the vectors and matrices in Equations (6)–(14), which are adequate for the scenario in Figure 2.

Firstly, the vectors and matrices of $E_l^{(i)}$ in Equation (6) for the scenario are of the following forms:

$$[d^{(i)}]_{4 \times 4} = \begin{bmatrix} 1000 \\ 0100 \\ 0010 \\ 0001 \end{bmatrix}, \quad (15)$$

$$[E_m^{(i)}(0)]_{4 \times 1} = \begin{bmatrix} E_1^{(i)}(0) \\ E_2^{(i)}(0) \\ E_3^{(i)}(0) \\ E_4^{(i)}(0) \end{bmatrix}, \quad (16)$$

$$[sc^{(i)}]_{4 \times 4} = \begin{bmatrix} 0011 \\ 0011 \\ 0011 \\ 0001 \end{bmatrix}, \quad (17)$$

$$[a_w^{(i)}]_{4 \times 4} = \begin{bmatrix} a_{w11}^{(i)} & a_{w12}^{(i)} & a_{w13}^{(i)} & a_{w14}^{(i)} \\ a_{w21}^{(i)} & a_{w22}^{(i)} & a_{w23}^{(i)} & a_{w24}^{(i)} \\ a_{w31}^{(i)} & a_{w32}^{(i)} & a_{w33}^{(i)} & a_{w34}^{(i)} \\ a_{w41}^{(i)} & a_{w42}^{(i)} & a_{w43}^{(i)} & a_{w44}^{(i)} \end{bmatrix}, \quad (18)$$

$$[a_s^{(i)}]_{4 \times 1} = \begin{bmatrix} a_{s1}^{(i)} \\ a_{s2}^{(i)} \\ a_{s3}^{(i)} \\ a_{s4}^{(i)} \end{bmatrix}. \quad (19)$$

Secondly, the vectors and matrices of $E_l^{(o)}$ in Equation (13) are of the following forms:

$$[d^{(o)}]_{5 \times 5} = \begin{bmatrix} 10000 \\ 01000 \\ 00100 \\ 00010 \\ 00001 \end{bmatrix}, \quad (20)$$

$$[E_j^{(o)}(0)]_{5 \times 1} = \begin{bmatrix} E_1^{(o)}(0) \\ E_2^{(o)}(0) \\ E_3^{(o)}(0) \\ E_4^{(o)}(0) \\ E_5^{(o)}(0) \end{bmatrix}, \quad (21)$$

$$[sc^{(o)}]_{5 \times 4} = \begin{bmatrix} 1111 \\ 1111 \\ 1111 \\ 0111 \\ 0111 \end{bmatrix}, \tag{22}$$

$$[a_w^{(o)}]_{4 \times 5} = \begin{bmatrix} a_{w11}^{(o)} & a_{w12}^{(o)} & a_{w13}^{(o)} & a_{w14}^{(o)} & a_{w15}^{(o)} \\ a_{w21}^{(o)} & a_{w22}^{(o)} & a_{w23}^{(o)} & a_{w24}^{(o)} & a_{w25}^{(o)} \\ a_{w31}^{(o)} & a_{w32}^{(o)} & a_{w33}^{(o)} & a_{w34}^{(o)} & a_{w35}^{(o)} \\ a_{w41}^{(o)} & a_{w42}^{(o)} & a_{w43}^{(o)} & a_{w44}^{(o)} & a_{w45}^{(o)} \end{bmatrix}, \tag{23}$$

$$[a_s^{(o)}]_{5 \times 1} = \begin{bmatrix} a_{s1}^{(o)} \\ a_{s2}^{(o)} \\ a_{s3}^{(o)} \\ a_{s4}^{(o)} \\ a_{s5}^{(o)} \end{bmatrix}. \tag{24}$$

Thirdly, the vectors and matrices of $E_l^{(e)}$ in Equation (14) have the following forms:

$$[d^{(e)}]_{7 \times 7} = \begin{bmatrix} 1000000 \\ 0100000 \\ 0010000 \\ 0001000 \\ 0000100 \\ 0000010 \\ 0000001 \end{bmatrix}, \tag{25}$$

$$[E_k^{(e)}(0)]_{7 \times 1} = \begin{bmatrix} E_1^{(e)}(0) \\ E_2^{(e)}(0) \\ E_3^{(e)}(0) \\ E_4^{(e)}(0) \\ E_5^{(e)}(0) \\ E_6^{(e)}(0) \\ E_7^{(e)}(0) \end{bmatrix}, \tag{26}$$

$$[sc^{(e)}]_{7 \times 4} = \begin{bmatrix} 1111 \\ 1111 \\ 1111 \\ 1111 \\ 1111 \\ 1111 \\ 1111 \end{bmatrix}, \tag{27}$$

$$[a_w^{(e)}]_{4 \times 7} = \begin{bmatrix} a_{w11}^{(e)} & a_{w12}^{(e)} & a_{w13}^{(e)} & a_{w14}^{(e)} & a_{w15}^{(e)} & a_{w16}^{(e)} & a_{w17}^{(e)} \\ a_{w21}^{(e)} & a_{w22}^{(e)} & a_{w23}^{(e)} & a_{w24}^{(e)} & a_{w25}^{(e)} & a_{w26}^{(e)} & a_{w27}^{(e)} \\ a_{w31}^{(e)} & a_{w32}^{(e)} & a_{w33}^{(e)} & a_{w34}^{(e)} & a_{w35}^{(e)} & a_{w36}^{(e)} & a_{w37}^{(e)} \\ a_{w41}^{(e)} & a_{w42}^{(e)} & a_{w43}^{(e)} & a_{w44}^{(e)} & a_{w45}^{(e)} & a_{w46}^{(e)} & a_{w47}^{(e)} \end{bmatrix}, \tag{28}$$

$$\begin{bmatrix} a_s^{(e)} \end{bmatrix}_{7 \times 1} = \begin{bmatrix} a_{s1}^{(e)} \\ a_{s2}^{(e)} \\ a_{s3}^{(e)} \\ a_{s4}^{(e)} \\ a_{s5}^{(e)} \\ a_{s6}^{(e)} \\ a_{s7}^{(e)} \end{bmatrix}. \tag{29}$$

Taking into account the above matrix description, the *input data* is divided into two groups. The first group characterizing the phenomenon of the analyzed disturbances consists of the *basic data* contained in Equation (11) and Equation (12), and in further parts of the article in Equations (16), (18), (19), (21), (23), (24), (26), (28), and (29). Effective values of the interference field (measured or calculated or adopted for simulation) are observed in Equations (16), (21), and (26), and wall attenuation factors (calculated, measured, or adopted for simulation based on the manufacturer’s descriptions) are in Equations (18), (23), and (28). The attenuation factor of the space between the place where the source of the disturbance was determined and the point of impact of this disturbance (usually measured in accordance with the requirements described in [14]) is shown in Equations (19), (24), and (29). The second group consists of the *control data* contained in Equation (7) and Equation (9), and in further parts of the article in Equations (15), (17), (20), (22), (25), and (27). *Control data* expressing the contribution of individual sources of interference in the attenuation process according to the classification is adopted in Equation (1), according to the division into *internal disturbing signals*, *external disturbing signals*, and *extraneous disturbing signals*, which are included respectively in Equations (15), (20), and (25). The *Control data* expressing the ratio of individual walls of the ship structure in the attenuation process, also according to the above classification, are included respectively in Equations (17), (22), and (27).

The calculated *output data* from Equations (6), (13), and (14) are used to calculate the final RMS value using Equation (1).

4. Verification of the Measurements from the EMC Topological Model

In this section, the practical verification of the described EMC topological matrix model is analyzed. The verification was made in situ (in an actual ship’s environment) as an example of the possibility of testing a real-life scenario, as shown in Figure 3 [14].

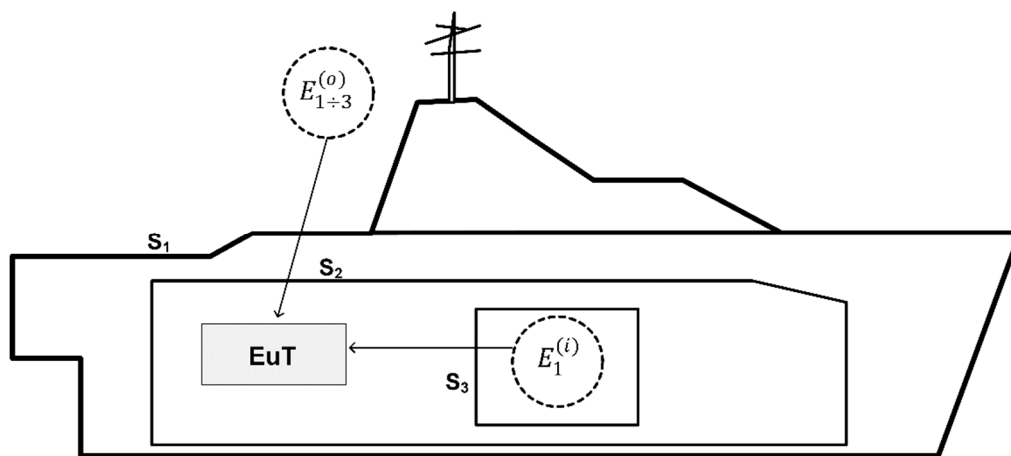


Figure 3. The practical scenario for the verification of in situ measurements.

In this scenario, the EuT is located in a subspace (the radio station room) surrounded by shielding plane S_2 and disturbed by four EM signals, which are as follows:

- $E_1^{(i)}$ is the ship's own internal disturbing signal, at a frequency of 29.5 MHz, from a radio amplifier surrounded by the shielding plane S_3 , which is situated under the main deck in the radio station room. The signal propagates to the EuT only via this plane;
- $E_1^{(o)}$ is the first external disturbing signal, which propagates at a frequency of 2 MHz from the transmitting antenna, and is situated above the main deck to the EuT via shielding planes S_1 and S_2 ;
- $E_2^{(o)}$ is the second external disturbing signal, which propagates at a frequency of 3025 MHz from the navigation radar antenna to the EuT in a similar way as above, via the shielding planes S_1 and S_2 ;
- $E_3^{(o)}$ is the third external disturbing signal, which propagates at a frequency of 9325 MHz from the navigation radar antenna to the EuT in a similar way as above, also via the shielding planes S_1 and S_2 .

At first, a theoretical EMC investigation of this scenario by applying the EMC topological model is performed. This requires a calculation of the effective value $E_I^{(t)}$ of the total disturbing signal at the EuT by using Equation (1). Consequently, this requires calculation of both resultant values of the internal and the external disturbing signals, i.e., $E_I^{(i)}$ and $E_I^{(o)}$, respectively, using Equation (2) and Equation (3). In turn, this requires calculation of the components of these signals, i.e., $E_{I1}^{(i)}$, $E_{I1}^{(o)}$, $E_{I2}^{(o)}$, and $E_{I3}^{(o)}$, by solving Equation (6) and Equation (13).

For this, we need to know:

- the source values of these signals, i.e., $E_1^{(i)}(0)$, $E_1^{(o)}(0)$, $E_2^{(o)}(0)$, and $E_3^{(o)}(0)$;
- the attenuation values of the shielding planes, i.e., $a_{w31}^{(i)}$, $a_{w11}^{(o)}$, $a_{w12}^{(o)}$, $a_{w13}^{(o)}$, $a_{w21}^{(o)}$, $a_{w22}^{(o)}$, and $a_{w23}^{(o)}$;
- the attenuation values of the disturbing signals in space, i.e., $a_{s1}^{(i)}$, $a_{s1}^{(o)}$, $a_{s2}^{(o)}$, and $a_{s3}^{(o)}$.

The values of the source's disturbing signals were measured during activation of the mentioned sources of EM disturbances. These values were as follows: $E_1^{(i)}(0) = 70 \text{ dB}\mu\text{V/m}$, $E_1^{(o)}(0) = 160 \text{ dB}\mu\text{V/m}$, $E_2^{(o)}(0) = 154 \text{ dB}\mu\text{V/m}$, and $E_3^{(o)}(0) = 146 \text{ dB}\mu\text{V/m}$.

The attenuation characteristics of the shielding planes (walls), S_1 , S_2 , and S_3 , with the points of the attenuation values a_w of the specified shielding planes for the selected frequencies of the marked disturbing signals, are presented in Figure 4. These characteristics are measured for perpendicular orientation of the measuring signal trajectory relative to the plane of the shielding surface.

$$E_1^{(i)} = E_{I1}^{(i)} = 70 \text{ dB}\mu\text{V/m} - 60 \text{ dB} - a_{s1}^{(i)} = 10 \text{ dB}\mu\text{V/m} \quad (30)$$

The in situ verification tests included measurements of elements of Equation (6) and Equation (13), which are expressed respectively by Equation (30) and Equation (31).

The total values of the attenuation a_s of the disturbing signals in the space between their sources and the EuT, taking into account the subspaces between the shielding planes, are calculated. These values are as follows: $a_{s1}^{(i)} \approx 0$, due to the space's short distance, and $a_{s1}^{(o)} = a_{s2}^{(o)} = a_{s1}^{(o)} = a_{s3}^{(o)} = 15.5 \text{ dB}$, due to the space's total distance, which was equal to 4.5 m.

Taking into account the above, for the scenario presented in Figure 3, the resultant value of the internal disturbing signal $E_I^{(i)}$, as seen in Equation (2), at the EuT has the one component, i.e., where $a_{s1}^{(i)} \approx 0$.



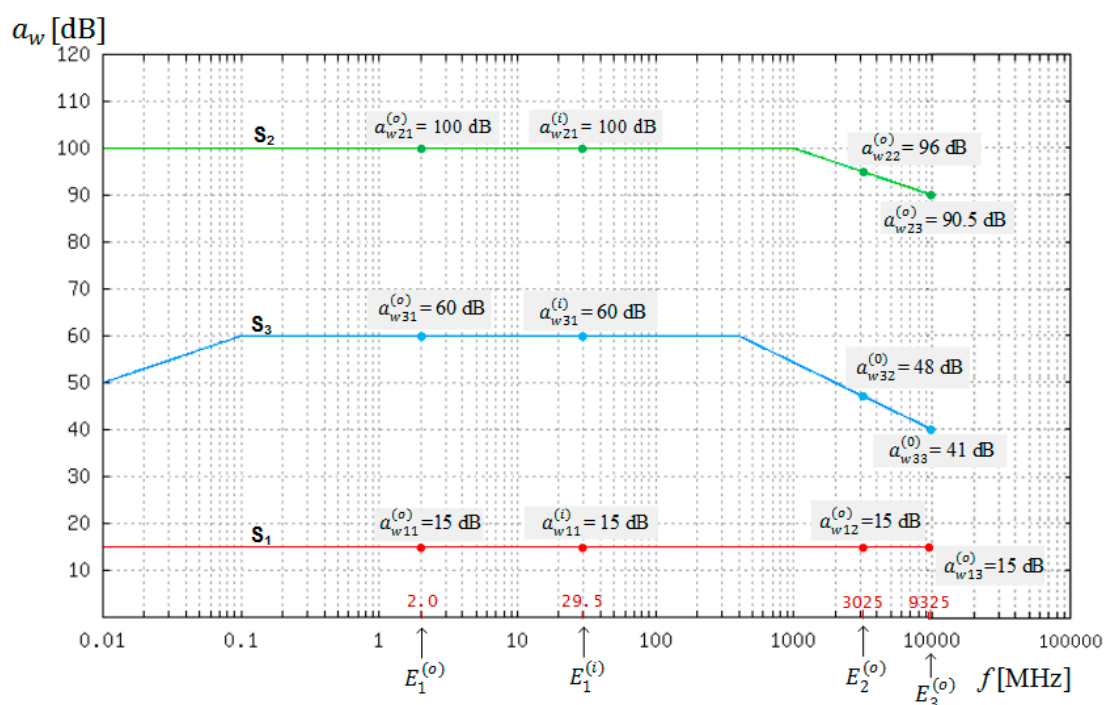


Figure 4. The attenuation characteristics of the shielding planes from Figure 3.

The values of the components of the external disturbing signal $E_l^{(o)}$, as seen in Equation (3), can be calculated by (13), which has the following form:

$$\begin{bmatrix} E_1^{(o)} \end{bmatrix} = \begin{bmatrix} E_{11}^{(o)} \\ E_{12}^{(o)} \\ E_{13}^{(o)} \end{bmatrix} = \begin{bmatrix} 100 \\ 010 \\ 001 \end{bmatrix} \cdot \begin{bmatrix} 160 \text{ dB}\mu\text{V/m} \\ 154 \text{ dB}\mu\text{V/m} \\ 146 \text{ dB}\mu\text{V/m} \end{bmatrix} - \begin{bmatrix} 115 \text{ dB} \\ 111 \text{ dB} \\ 105.5 \text{ dB} \end{bmatrix} - \begin{bmatrix} 15.5 \text{ dB} \\ 15.5 \text{ dB} \\ 15.5 \text{ dB} \end{bmatrix} = \begin{bmatrix} 29.5 \text{ dB}\mu\text{V/m} \\ 27.5 \text{ dB}\mu\text{V/m} \\ 25 \text{ dB}\mu\text{V/m} \end{bmatrix}. \quad (31)$$

Practically, the best way to verify the correctness of the EMC topological model is to compare the values of the disturbing signals at the EuT, i.e., $E_{11}^{(i)}$, $E_{11}^{(o)}$, $E_{12}^{(o)}$, and $E_{13}^{(o)}$, which can be calculated by using the model to measure their values using a spectrum analyzer.

The theoretical values calculated by the EMC topological model and the values in situ measured using a spectrum analyzer of all the disturbing signals at the EuT are compared and expressed in Figure 5, where the lines show the values measured by the spectrum analyzer and the circles show the values calculated by using the described topological model.

For practical reasons, the obtained number of test results is small due to the limited number of measurements on an operating navy ship. However the results of these measurements are unique on a global scale. The smallest difference between the calculated (25 dB μ V/m) and measured (24 dB μ V/m) values of the same disturbing signal, i.e., ($E_{13}^{(o)}$) at the EuT, is 0.9 dB, or 3.7%. These results are acceptable. However, the largest difference between the calculated (29.5 dB μ V/m) and measured (36.5 dB μ V/m) values of the same signal, i.e., ($E_{11}^{(i)}$) at the EuT, is 7 dB, or 19%, which is relatively high.

Such a discrepancy in the results is influenced by the complexity and tightness of the ship's construction. However, simulation studies using this model allow us to analyze variations in the location of a ship's devices and systems that are sensitive to EM disturbances. This allows us to develop an optimal solution in this respect. Often, it is not important to accurately determine the value of a disturbing signal at the selected location of the EuT, but the identification of where this signal will potentially be the smallest allows us to determine the best EuT location. Due to time and cost constraints, such an approach is the only one that is acceptable in the practice of a ship's exploitation or the rebuilding of a ship's electrical and electronic equipment.

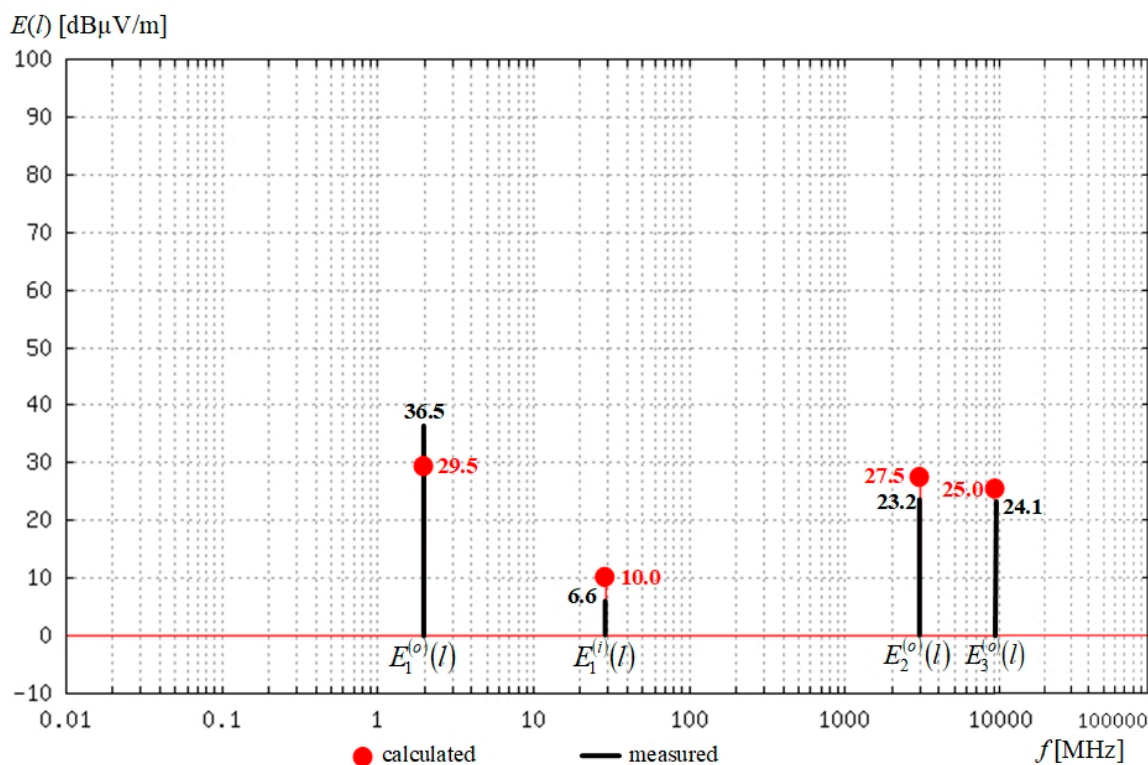


Figure 5. The comparison of the calculated and measured values of the disturbing signals at the equipment under test (EuT).

Summarizing the results of the comparison and taking into account practical aspects, especially the complex character of EMC investigations, we conclude that the EMC topology model is useful for practical applications, particularly when designing studies regarding the optimal locations for a ship's electrical and electronic equipment.

5. Conclusions

This article considered the problem of analysis of the electromagnetic compatibility in a ship's environment. This problem is important to consider and has an impact on people's safety and the ship's operation. Currently, techniques and ship technologies are characterized by the use of complex systems and electronic devices, including radio communication and radio navigation systems. The electronic systems and devices for automatic control of the ship's functions are particularly sensitive in this respect. Usually, they operate at relatively low energy levels and are sensitive to electromagnetic disturbances.

In this paper, the problem concerning EM interactions between electrical and electronic devices in a naval ship's environment are analyzed. These devices radiate EM fields that have a mutual influence on their operation, thereby disturbing their operation properties. This problem is important to consider because it is vital that these devices work effectively. The described method has important utility for analyzing EMC conditions when designing a ship's internal structure, the deployment of energetic equipment and radio and navigation devices, and electronic elements of the ship's control systems.

To analyze and solve the problem, a new computational model in the form of a matrix equation set is proposed. In the model, the ship's internal structure (under the main deck) and the locations of the sources of disturbing signals are taken into account. The ship's topological structure and its EMC topological model are described. Classification of the disturbing signals in a real naval ship scenario is shown.

An example application of the matrix description and verification of the measurements in an in situ naval ship scenario are also presented. This verification confirms the usefulness of the proposed model in the design and exploitation of naval ship operations. For example, this helps to determine

the kind of shielding planes (walls) that can be applied to effectively protect electrical and electronic ship devices against EM disturbances. It can be applied to the modernization of a ship structure's exploitation to obtain better EMC conditions, and also to improve the safe functioning of electrical and electronic equipment.

Moreover, the described topological matrix EMC model can be used in simulation investigations of extraneous EM disturbances.

Author Contributions: All authors contributed to developing the measurement equipment, designing and performing measurements, data analysis, scientific discussions, and writing the paper.

Funding: This research received no external funding.

Acknowledgments: This work was performed with financial support from the Faculty of Electronics, Telecommunications, and Informatics of Gdansk University of Technology and the R&D Marine Technology Centre in Gdynia, Poland.

Conflicts of Interest: The authors have no conflict of interest to declare.

References

1. Tesche, F.M. Topological concept for internal EMP interaction. *IEEE Trans. Electromagn. Compat.* **1978**, *EMC-20*, 60–64. [[CrossRef](#)]
2. Baum, C.E. Electromagnetic topology for the analysis and design of complex electromagnetic systems. In *Fast Electrical and Optical Measurements*; Thompson, I.E., Luessem, L.H., Eds.; Martinus Nijhoff: Dordrecht, The Netherlands, 1986; Volume I.
3. Parmantier, J.P.; Gobin, V.; Issac, F. Application of EM topology on complex systems. In Proceedings of the 1993 IEEE EMC Symposium, Dallas, TX, USA, 9–13 August 1993.
4. Agee, F.J.; Kirawanich, P.; Yakura, J.; Tzeremes, G.; Christodoulou, C.; Islam, N.E. An electromagnetic topology based simulation for wave propagation through shielded and semi-shielded systems following aperture interactions. *WIT Trans. Model. Simul.* **2005**, *41*, 601–610.
5. Catryse, J. Architectural shielding: From needs into practical realization. In Proceedings of the XIVth International Wroclaw Symposium and Exhibition on Electromagnetic Compatibility, Wroclaw, Poland, 14–18 September 1998; pp. 407–410.
6. Katulski, R.J.; Dymarkowski, K.; Namiotko, R. Protection system against electromagnetic leak of information. In Proceedings of the IEEE International Conference on Homeland Security, Boston, MA, USA, 7 June 2006.
7. Namiotko, R. Emmisivity Investigations of Devices and Systems in the Ship EM Environment. Ph.D. Thesis, National Institute of Telecommunications, Warsaw, Poland, 2007. (In Polish).
8. Paul, C.R. *Introduction to Electromagnetic Compatibility, Part II: Application to EMC Design*; John Wiley & Sons, Inc.: Hoboken, NJ, USA, 1992.
9. IEEE Std 299-1997. *IEEE Standard Method for Measuring the Effectiveness of Electromagnetic Shielding Enclosures*; Standard Committee of the IEEE Electromagnetic Compatibility Society: Piscataway, NJ, USA, 1997. [[CrossRef](#)]
10. STANAG 4557. *EM Shielding: Methods of Standard Attenuation Measurements for Naval Enclosures*; NATO Standardization Agreement: Brussels, Belgium, 2001.
11. STANAG 4435. *Electromagnetic Compatibility Testing Procedure and Requirements for Naval Electrical and Electronic Equipment*; NATO Standardization Agreement: Brussels, Belgium, 1993.
12. Horn, R.A.; Johnson, C.R. *Topics in Matrix Analysis, Chapter 5: The Hadamard Product*; Cambridge University Press: Cambridge, UK, 1994.
13. EN 55016+203. *2010 Specification for Radio Disturbance and Immunity Measuring Apparatus and Methods, Part 2–3: Methods of Measurement of Disturbances and Immunity—Radiated Disturbance Measurements*; Polish Committee for Standardization (PKN): Warsaw, Poland, 2010.
14. AECTP-500. *Electrical/Electromagnetic Tests*; NATO: Brussels, Belgium, 2004.



© 2019 by the authors. Licensee MDPI, Basel, Switzerland. This article is an open access article distributed under the terms and conditions of the Creative Commons Attribution (CC BY) license (<http://creativecommons.org/licenses/by/4.0/>).